THERMOMECHANICAL PROPERTIES OF SHAPE MEMORY ALLOYS AND POLYMERS STUDIED BY ADVANCED INFRARED TECHNIQUES

Pieczyska Elżbieta, epiecz@ippt.pan.pl
Maj Michał, mimaj@ippt.pan.pl
Staszczak Maria, mstasz@ippt.pan.pl
Kowalczyk-Gajewska Katarzyna, kkowalcz@ippt.pan.pl
Institute of Fundamental Technological Research PAS, Pawinskiego 5B, 02-106 Warsaw, Poland

Tobushi Hisaaki, tobushi@aitech.ac.jp
AICHI Institute of Technology, Toyota-city, Japan

Shuichi Hayashi, hayashi@smptechno.com
SMP Technologies Inc., Tokyo, Japan

Abstract. *The paper presents experimental evaluation and modelling of effects of thermomechanical couplings in shape memory alloy (SMA) and shape memory polymer (SMP). TiNi SMA and polyurethane PU-SMP are subjected to tension on MTS Testing machine. Fast infrared camera (IR) Phoenix FLIR System enable obtaining temperature distribution and average temperature changes of the specimens during the deformation process.*
Mechanical and infrared characteristics recorded during the SMA loading show that after initial, macroscopically homogeneous deformation a localized transformation develops, accompanied by significant temperature changes. Inclined bands of higher temperature accompanying exothermic forward transformation are recorded during the loading, whereas bands of lower temperature related to endothermic reverse transformation are observed during the unloading process. The infrared imaging and average temperature of the SMA sample compared to their mechanical characteristics allow to investigate the current stage of the stress-induced transformation process. A decrease of the specimen temperature reveals the saturation stage of the transformation. Both mechanical and thermal effects significantly depend on the strain rate; the higher the strain rate, the higher the temperature and stress are obtained.
Similar experimental methodology is applied to investigate effects of thermomechanical couplings in shape memory polyurethane subjected to tension at various strain rates. Constitutive model valid in finite strain regime is proposed, where the SMP is described as a two-phase material composed of hyperelastic rubbery phase and elastic-viscoplastic glassy phase, while the volume content of phases is specified by the current temperature. Experimental results and modelling show that the SMP deformation process strongly depends on the strain rate, much stronger than for metals and alloys. At higher strain rate higher stress and temperature changes are obtained, since the deformation process is more dynamic and occurs in almost adiabatic conditions. It is shown that during the SMP loading process various deformation mechanisms are active at various strain rates.

Keywords*: shape memory alloy, transformation bands, shape memory polymer, infrared camera, constitutive model*

1. INTRODUCTION

In order to contribute to solving the problems of natural resources, energy and environment protection of the earth, the development of multifunctional smart materials and structures is required. In the intelligent materials, investigation of shape memory alloys and shape memory polymers has attracted high attention due to their functional properties and huge potential in practical applications. In SMA, the shape memory property appears based on the reversible martensitic transformation in which the crystal structure varies depending on the variation in stress or temperature (Tobushi *et al*., 2013, Pieczyska *et al*., 2013, Pieczyska, 2010). In SMP, the shape memory property appears based on the radical difference of its elastic modulus and yield point below and above the glass transition temperature: the elastic modulus is high at the temperature below and low at temperatures above T_g. Such behavior is caused by significant change of the molecular motion at temperature (Tobushi *et al*., 2013, Hayashi, 1993). Among the shape memory polymers, the polyurethane has been most often practically used (Huang *et al*., 2012). In this paper, development of stress-induced martensitic transformation in TiNi SMA and thermomechanical behavior of PU-SMP in tension are presented.

2. EXPERIMENTAL DETAILS

The shape memory material specimens are mechanically loaded on MTS 858 testing machine at room temperature. Furthermore, fast and sensitive FLIR Co infrared camera is used in order to measure effects of thermomechanical coupling accompanying the stress-induced martensitic transformation process in TiNi shape memory alloy and effects of thermomechanical couplings in shape memory polyurethane. Scheme of the experimental set-up is shown in Fig. 1a. A shape memory polyurethane sample in grips of testing machine is presented in Fig. 1b.

a) b)

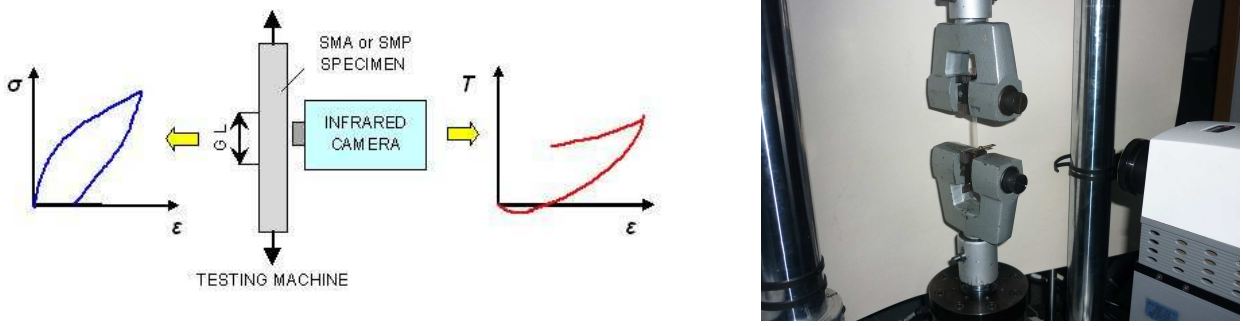

Figure 1. a) Schematic of experimental set-up for investigation of shape memory polymer mechanical and temperature characteristics; b) shape memory polyurethane sample in grips of testing machine

a) b)

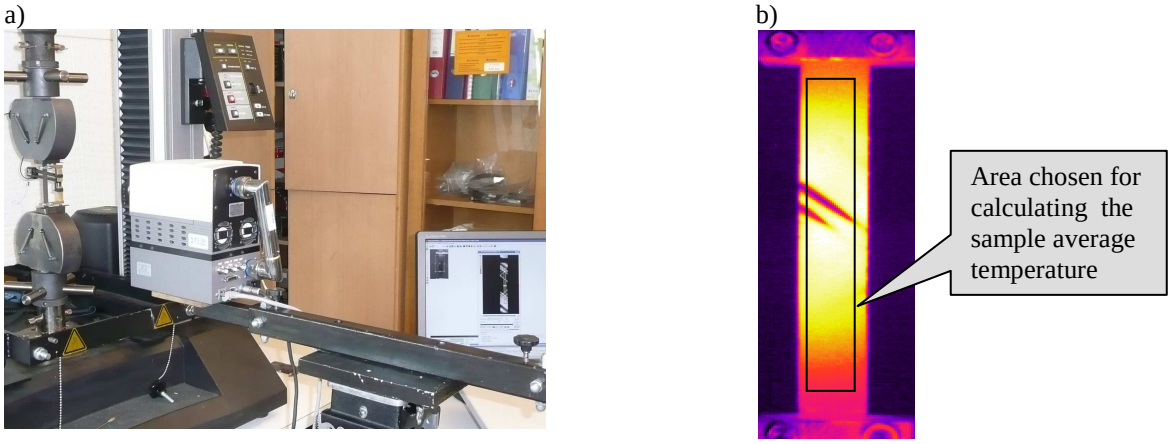

Figure 2. a) Photograph of shape memory alloy sample in grips of testing machine - monitor shows infrared image of transformation bands; b) thermogram showing chosen area for calculation the sample average temperature

Photograph of the shape memory alloy sample in grips of testing machine during the tension process is shown in Fig. 2b. On the monitor in the left an infrared image of the stress-induced transformation bands can be noticed. Infrared image of the SMA sample subjected to loading is presented in Fig. 2b. In addition, a rectangular shape on the sample surface was denoted showing chosen area for the sample average temperature calculation.

3. THERMOMECHANICAL PROPERTIES OF SHAPE MEMORY ALLOY

Stress-strain curve and their related average temperature changes calculated from the SMA sample for stress-controlled test in the case of stress rate 25 MPa/s are shown in Fig. 3. Conditions of nucleation, development and saturation of the stress-induced martensitic transformation were studied, basing on the SMA specimen temperature distribution and its temperature changes. It was found that the initial phase transformation is macroscopically homogeneous and it occurs before the stress-strain knee, while in the yield point area bands of localized transformation occur, characterized by a much higher temperature than the other parts of the specimen. At higher strain, more and more such bands develop and overlap, leading to a significant increase in the average sample temperature, followed by an increase of the transformation stress. In the final part of the SMA loading a decrease of the average sample temperature was recorded which revealed the saturation stage of the exothermic martensitic forward transformation.

The bands of significantly higher temperature compared to the other part of the specimen ($\Delta T \cong 8$K) are infrared imaging of the SIMT, observed during the SMA loading, whereas the bands of lower temperature ($\Delta T \cong 6$K) are related to the reverse transformation, observed in the course of unloading. The bands of the newly emerged martensite/austenite phase are characterized by approximately 48° inclination angle formed with tension direction, though the slope depends on the specimen geometry (Pieczyska, 2010). Moreover, using the fast and sensitive infrared camera we have also noticed that at the advanced stage of martensitic forward/reverse transformation, a new generation of much thinner transformation bands can form. The fine bands nucleate in regular distances from the formerly developed much wider bands, creating “radiator-like” effects. They probably appear and develop in this part of the specimen in order to compensate the local stress-strain state instability, caused by the current loading and the transformation progress conditions (Pieczyska *et al*., 2013).

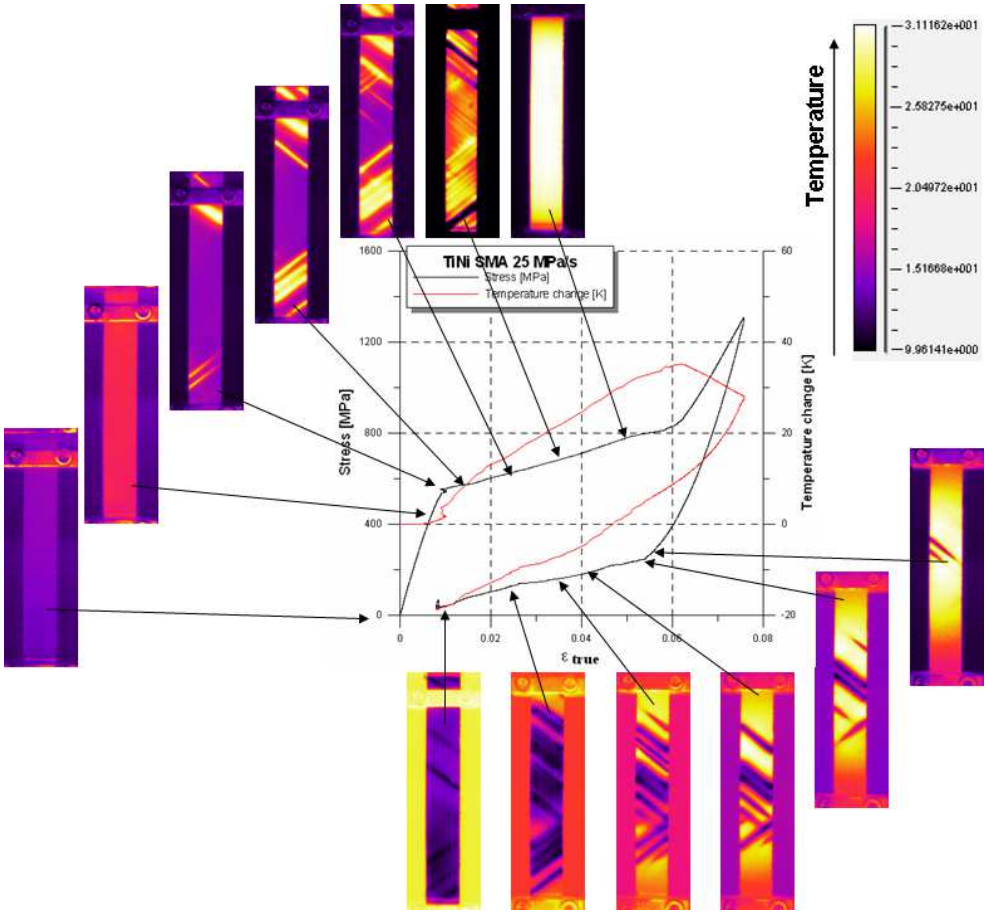

Figure 3. Stress and average temperature change vs. strain and infrared imaging of localized transformation bands recorded in TiNi shape memory alloy subjected to complete loading-unloading cycle at stress rate of 25 MPa/s.

Furthermore, it was observed that nucleation of the localized martensitic forward transformation takes place in the weakest area, whereas the reverse transformation always initiates in the central part of the SMA specimen.

4. THERMOMECHANICAL PROPERTIES OF SHAPE MEMORY POLYMER – EXPERIMENTAL RESULTS AND MODELLING

Investigation of thermomechanical coupling occurring during PU-SMP tension was performed at room temperature (23 ^{o}C) untill the sample rupture in order to learn more about the SMP thermomechanical behavior and to propose proper strain range in the following tests. Results obtained for the tension process performed with strain rate $2x10^{-2}s^{-1}$ is shown in Fig. 4. Photographs of the sample in grips of the testing machine recorded at subsequent stages of the deformation is shown in Fig. 4a, whereas the stress vs. strain curves is shown in Fig. 4b: the numbered stars denote the strain stages shown in Fig. 4a, respectively. The initial measurement base was only 15 mm, therefore it was not so easy to rupture the thoroughly prepared SMP sample. The stress and strain quantities are related to the current (instantaneous) values of the sample cross-section, obtaining so-called “true stress” and “true strain” values, presented in the diagrams (Figs 4, 5).

From a dynamic mechanical analysis (DMA) performed in tension with frequency of force 1 Hz and heating rate of 2°C/min the SMP parameters were estimated: glass transition temperature Tg = 25 MPa, elastic modulus Eg' = 1500, rubber modulus Er'= 15 MPa. The obtained results confirm the SMP good shape memory properties. The initial tension of SMP was accompanied by a small drop in temperature, related to the SMP yield point, called thermoelastic effect. At higher strains, the stress and temperature significantly increase due to reorientation of the polymer molecular chains.
Until the true strain value equal to approximately 1.5 the SMP exhibits a smooth, hardening-like behaviour. The “hardening” is a result of the reorientation of the polyurethane molecular chains that can induce nucleation of voids or even the polymer structure crystallization which can be observed as the sample whitening (Fig. 4a; photograph 4). For the strain rate 2×10^{-2} s^{-1} the SMP deformation process is almost isothermal; the maximal temperature change estimated for the sample rupture is only 3K. However, the polymers are very sensitive to strain rates. Comparison of the experimental results and modelling for various strain rates, i.e. true stress versus true strain obtained during tension with

strain rates $2x10^{-1}s^{-1}$, $2x10^{0}s^{-1}$ and $1x10^{1}s^{-1}$ are shown in Fig. 7 (a), and their related temperature changes in Fig. 7 (b). The higher the strain rate, the higher the temperature changes obtained, since the deformation process is more dynamic and occurs in the conditions close to adiabatic. The maximal temperature changes estimated by infrared camera computer system at higher strain rates are as follows: 18 K for $2x10^{-1}s^{-1}$, 37 K for $2x10^{0}s^{-1}$ and 44 K for $10^{1}s^{-1}$. The obtained elongation limit of the SMP is over 180 % as measured as true strains.

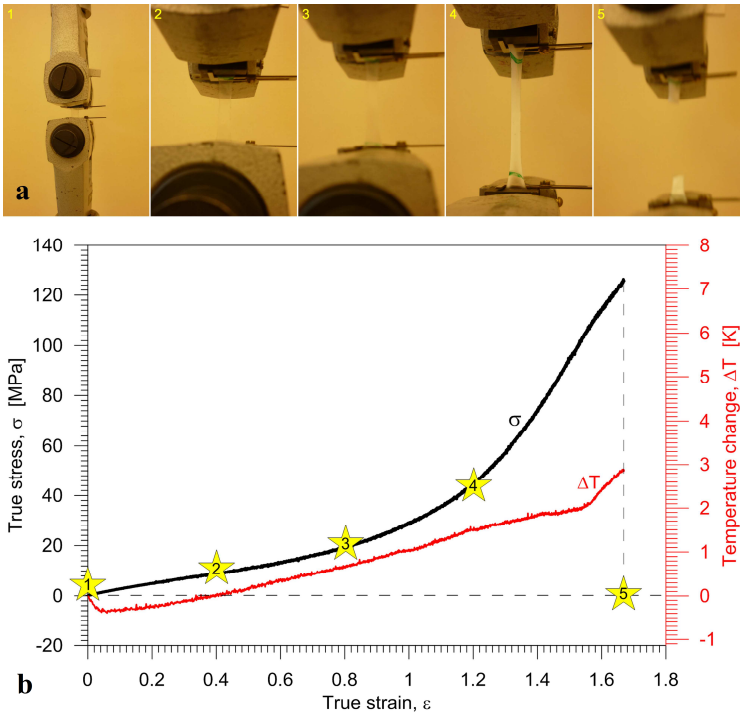

Figure 4 a) PU-SMP sample in grips of testing machine showing subsequent stages of the tensile process 1-4. b) Stress and temperature changes vs. strain for strain rate $2x10^{-2}s^{-1}$: stars show strain stages presented in the photographs above.

There are two modelling frameworks developed for SMP: phase transition approach and thermo-viscoelastic approach, cf. (Nguyen *et al.*, 2010). The first approach is employed in this paper. According to our proposal, SMP is assumed to be a mixture of two phases: a soft rubbery phase and a hard glassy phase. Such modelling approach is well justified by the physical features of the analyzed polyurethanes: the presence of soft and hard segments and the separation of the domains dominated by respective phases. Following Qi *et al.*, (2008), the volume fraction of each phase within the representative volume of the material is postulated as a logistic function of temperature (Fig. 5)

$$f_r = \frac{1}{1+\exp(-(T-T_r)/A)}, \quad f_g = 1 - f_r \tag{1}$$

The material parameter A and the reference temperature T_r, related to the glass transition temperature T_g, are identified using variation of a storage modulus with temperature obtained in DMA of the PU-SMP.

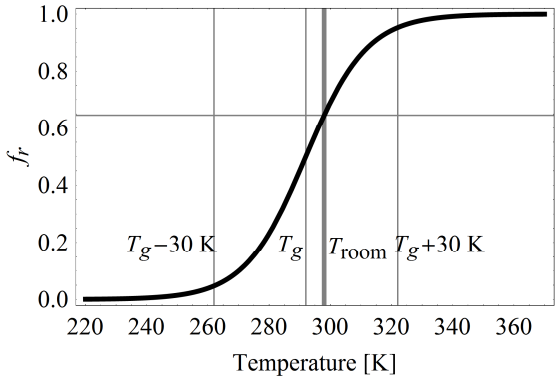

Figure 5. Assumed dependency of volume fraction of rubbery phase f_r on temperature in the PU-SMP volume element.

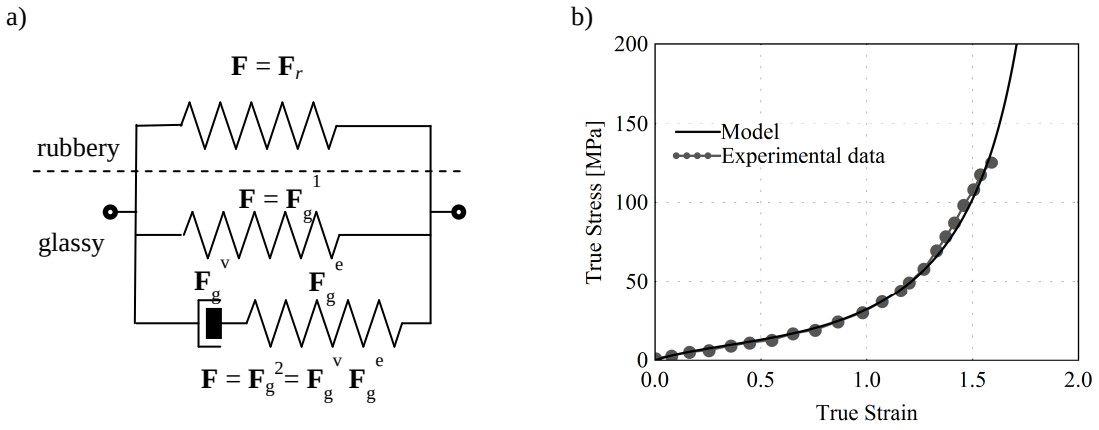

Figure 6. a) Schematic representation of the constitutive model of PU-SMP, b) Stress versus strain for SMP tension till rapture with strain rate $2x10^{-2}s^{-1}$. Comparison of model predictions and experimental results.

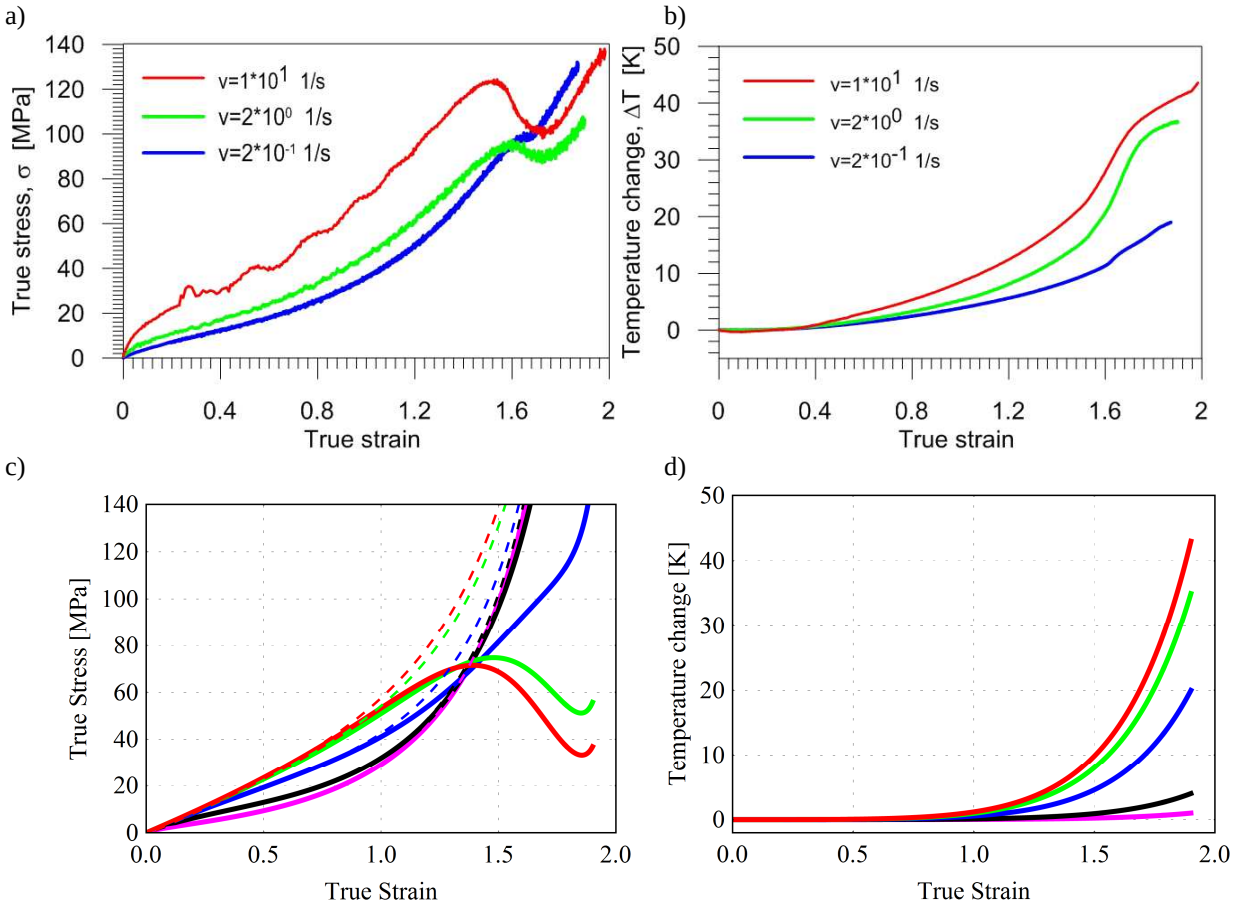

Figure 7. Stress vs. strain (a) and temperature change vs. strain (b) for PU-SMP tension with various strain rates; together with the model predictions (c) for the temperature variation (d). Notation for colors is the same as in (a) and (b). Additionally results obtained for strain rates $2x10^{-2}s^{-1}$ (black, cf. Fig. 6b) and $2x10^{-3}s^{-1}$ (magenta) are shown.

Constitutive equations are formulated separately for each phase within the large strain format, following Qi *et al.* (2008) proposal (see Fig. 6a). The Cauchy stress $\boldsymbol{\sigma}_r$ in the rubbery phase is related to the deformation gradient of this phase $\mathbf{F}_r$ according to the hyperelastic Aruda-Boyce eight chain model (A-B), while the glassy phase is hyperelastic-viscoplastic with the Zener-type behavior. The stress $\boldsymbol{\sigma}_g^{\,1}$ is related to $\mathbf{F}_g^{\,1}$ again by the hyperelastic A-B model (with different parameters than for the rubbery phase) and the stress $\boldsymbol{\sigma}_g^{\,2}$ is related to $\mathbf{F}_g^{\,e}$ by the neo-Hook relation with the logarithmic strain measure. The equivalent viscoplastic shear rate in the glassy phase depends on the equivalent Huber-von Mises stress, calculated for the stress tensor $\boldsymbol{\sigma}_g^{\,2}$, according to the power-law (compare the 1D model due to Tobushi *et al.*, (2001)),

$$\dot{\gamma}_v = \dot{\gamma}_0 \left| \frac{\tau_{gv}}{\tau_{gv}^c} \right|^{m+1} \quad \text{, where } \tau_{gv}^c = \tau_{sat} + (\tau_0 - \tau_{sat}) \exp(-b\gamma_v) \tag{2}$$

and $\dot{\gamma}_0$ is a reference shear rate, m - an exponent describing the degree of strain rate sensitivity while τ^c_{gv} - a critical shear stress. Constants τ_0, τ_{sat} and b are additional material parameters describing evolution of τ^c_{gv} with the accumulated viscoplastic deformation γ_v. The material parameters present in the model were preliminarily identified through tension tests until rupture at strain rates of $2\text{x}10^{-3}\text{s}^{-1}$ and $2\text{x}10^{-2}\text{s}^{-1}$. The resulting behavior of the material depends on the actual material composition. At this stage simple Voigt-type averaging scheme is used, i.e. each phase is supposed to share the same deformation gradient **F** being equal to the macroscopic one, while the total Cauchy stress tensor $\boldsymbol{\sigma}$ in the material is an average of stresses in the individual phases. Refined averaging schemes developed for two-phase elastic-viscoplastic materials, cf. (Kowalczyk-Gajewska and Petryk, 2011), can be used in order to obtain more realistic redistribution of stresses and strains between phases.

Simulations were carried out of tension tests until rupture. Comparison with experimental results for the strain rate of $2\text{x}10^{-2}\text{s}^{-1}$ is shown in Fig. 6b. For the assumed material parameters the model correctly predicts the elongation limit and the level of stress. Temperature change observed in the experiment for this strain rate is not significant. Contrary, considerable increase of temperature with respect to the ambient temperature is observed at higher strain rates (see Fig. 7b), associated with the rapid accumulation of viscoplastic deformation. Preliminary verification of the formulated model has been conducted for higher strain rates assuming non-isothermal conditions of the process. A temperature evolution with strain, shown in Fig. 7d, is used as an input data in simulations. It roughly approximates the temperature change observed experimentally (compare Fig. 7b and 7d). In Fig. 7c the effect of temperature change can be assessed by comparing the stress-strain curves obtained, taking into account the temperature evolution with the results obtained under the assumption of constant temperature, shown by dashed lines of the same color. The model predicts qualitatively the observed decrease in stress at higher strain rates associated with the temperature increase and, consequently, with the increase of a volume content of the soft rubbery phase in the sample. However, the reduction of the stress level predicted by the model is stronger than the one observed experimentally (compare Fig. 7a and 7c). Model predictions can be improved by a more detailed analysis of thermomechanical couplings and the refined identification of model parameters performed using the experiments conducted at temperatures well below and well above glass transition temperature for separate characterization of mechanical response of two phases.

3. ACKNOWLEDGEMENTS

The research has been carried out with support of the Polish National Center of Science under Grant No. 2011/01/M/ST8/07754. Authors are grateful to Dr. Mariana Cristea for elaborating the PU-SMP dynamic mechanical analysis and valuable comments, to Leszek Urbański for obtaining mechanical data and to Paulina Pieczyska for linguistic corrections of the text.

4. REFERENCES

Tobushi, H., Matsui, R., Takeda, K. and Pieczyska, E., 2013. Mechanical Properties of Shape Memory Materials. Materials Science and Technologies, Mechanical Engineering Theory and Applications; NOVA Publishers.

Pieczyska, E., Tobushi, H., Kulasiński, K., 2013. Development of transformation bands in TiNi SMA for various stress and strain rates studied by a fast and sensitive infrared camera, Smart Materials & Structures, Vol. 22, 035007-1-8.

Pieczyska, E., 2010. Activity of stress-induced martensite transformation in TiNi shape memory alloy studied by infrared technique, Journal of Modern Optics, Vol. 57, 18, pp. 1700-1707.

Hayashi, S., 1993. Properties and Applications of Polyurethane-series Shape Memory Polymer, Int. Progress in Urethanes, Vol. 6, pp. 90 – 115.

Huang, W.M., Young, B. and Fu, Y.Q., 2012. Polyurethane Shape Memory Polymers, Taylor & Francis Group.

Nguyen, T.D., Yakacki, C.M., Brahmbhatt, P.D. and Chambers M.L., 2010. Modeling the relaxation mechanisms of amorphous shape memory polymers. Advance Materials, 22, pp. 3411–3423

Qi, H.J., Nguyen, T.D., Castro, F., Yakacki, C.M. and Shandas, R., 2008. Finite deformation thermomechanical behavior of thermally induced shape memory polymers. J. of Mechanics and Physics of Solids 56, pp. 1730-1751

Kowalczyk-Gajewska, K. and Petryk, H., 2011. Sequential linearization method for viscous/elastic heterogeneous materials, European Journal of Mechanics A/Solids 30, pp. 650–64

Tobushi, H., Okumura, K., Hayashi, S. and Ito, N., 2001. Thermomechanical constitutive model of shape memory polymer, Mechanics of Materials, 33, pp. 545-554.

5. RESPONSIBILITY NOTICE

The authors are the only responsible for the printed material included in this paper.